



Dedicated to Dr. Maria Zaharescu
on the occasion of her 85th anniversary

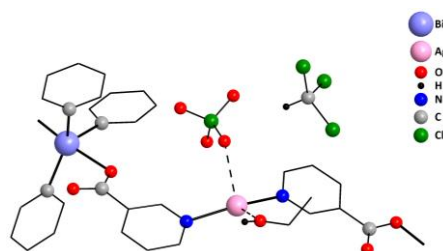
[Ag(EtOH){Ph₃Bi[O(O)CC₅H₄N-3]₂}](ClO₄)·CHCl₃ – A COORDINATION POLYMER BASED ON A DIVERGENT, DITOPIC METALLOLIGAND**

Ahmad BEN KIRAN, Anca SILVESTRU, Ciprian I. RAT* and Cristian SILVESTRU*

Supramolecular Organic and Organometallic Chemistry Centre, Department of Chemistry, Faculty of Chemistry and Chemical Engineering, Babeș-Bolyai University, 11 Arany Janos Str., RO-400028 Cluj-Napoca, Roumania

Received April 25, 2022

Reaction of Ph₃Bi[O(O)CC₅H₄N-3]₂ (**1**) in CHCl₃ and AgClO₄ in ethanol, in 1:1 molar ratio, afforded the isolation of colorless crystals of a coordination compound which was proved to be [Ag(EtOH){Ph₃Bi[O(O)CC₅H₄N-3]₂}](ClO₄)·CHCl₃ (**2·CHCl₃**) by single-crystal X-ray diffraction. A 1D coordination polymer is formed based on bridging triphenylbismuth(V) di(nicotinate) between silver atoms, with *trans* Ag–N dative bonds [2.183(4), 2.196(5) Å]. Additional Ag···O interactions are established between the coinage metal atom and an ethanol molecule [2.58(3) Å] as well as a perchlorate anion [2.746(6) Å], respectively. Its supramolecular architecture, based on a variety of non-covalent interactions, *i.e.* O–H···O, C–H···O or C–H···Cl hydrogen bonds, π···π, C–H···π, C–Cl···π interactions, as well as Ag···O and Ag···Cl contacts, is discussed.



INTRODUCTION

A common, largely developed, strategy to obtain discrete or polymeric heterometallic compounds is the use of organic ligands with an appropriate design with respect to the number, type, and position of the connecting sites as linkers (building blocks) between metal atoms. Organometallic compounds with potential to behave as ligands for a metal center through either a variety of non-covalent bonds or strong dative bonds also represent an option to be considered for a straightforward pathway to heterometallic species, including both discrete oligomeric derivatives and coordination polymers.¹ Most common and quite extensively used are the commercially available

ferrocenecarboxylic² and 1,1'-ferrocenedicarboxylic acids,³ as well as a large variety of synthetic proligands containing a ferrocenyl fragment which can act either as anionic or neutral potential linkers.⁴ Examples of other organometallic compounds of transition metals reported as linkers or metallotectons for the synthesis of discrete heteronuclear species or coordination polymers of different dimensionalities are the $[(\eta^4\text{-benzoquinone})\text{Mn}(\text{CO})_3]^-$ anion,⁵ and the related neutral species $[(\eta^4\text{-dichalcogenobenzoquinone})\text{M}(\text{CsMe}_5)]$ (M = Rh, Ir),⁶ the square planar complexes containing *cis*- or *trans*-(4-PyC≡C)₂Pt(PEt₃)₂ or related fragments,⁷ or metal–NHC (carbene) complexes.⁸ By contrast, main group organometallic compounds were only

*Corresponding author: cristian.silvestru@ubbcluj.ro; ciprian.rat@ubbcluj.ro

** Supplementary information on: <https://www.icf.ro/rrch/> or <https://revrouuum.lew.ro>

scarcely used to build heterometallic coordination polymers. We have previously reported on coordination polymers of different dimensionalities based on bis(4-pyridyl)mercury(II) as a linear tecton, *i.e.* Cu(II),⁹ Mn(II), Ni(II) or Zn(II)¹⁰ complexes. Organotin(IV) compounds containing the same 4-pyridyl group as part of an organic ligand attached to the group 14 metal were used to prepare discrete Pd(II)/Sn(IV)¹¹ and Zn(II)/Sn(IV)¹² heterometallic species.

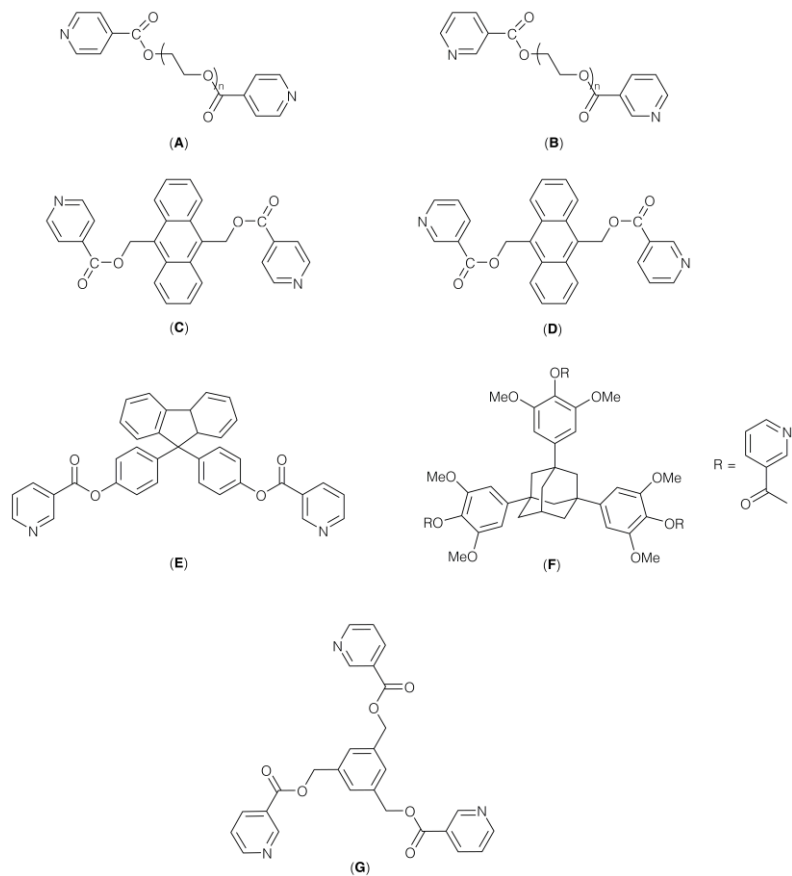


Chart 1

Recently, we have used the triphenylbismuth(V) derivatives of isonicotinic and nicotinic acids as divergent organometallogligands to build silver(I) coordination polymers and we observed a strong influence of the nature of the counteranion (triflate, nitrate or hexafluoroantimonate) on the supramolecular architecture built in solid state through a variety of non-covalent interactions ($\pi\cdots\pi$, Ag \cdots Ag, Ag \cdots O).¹

We report here on a new silver(I) coordination polymer, *i.e.* $[\text{Ag}(\text{EtOH})\{\text{Ph}_3\text{Bi}[\text{O}(\text{O})\text{CC}_5\text{H}_4\text{N}-3]_2\}(\text{ClO}_4)]\cdot\text{CHCl}_3$ (**2** \cdot CHCl_3), which exhibits a complex supramolecular architecture based on a variety of non-covalent interactions as proved by single-crystal X-ray diffraction.

Particular designed esters of isonicotinic and nicotinic acids as those depicted in Chart 1, with either flexible (**A–D**)¹³ or *quasi-rigid* (**E–G**)¹⁴ skeletons, were used to prepare silver(I) complexes and, depending on the nature of the ligand, anions and solvents, discrete rings,^{13a,e,f,14c} cages^{14d} as well as coordination polymers of silver(I),^{13a,b,d,e,f,14c,e} were obtained. For many such silver(I) complexes biological activity^{13c,f,15} or optical properties^{14a,b} were reported.

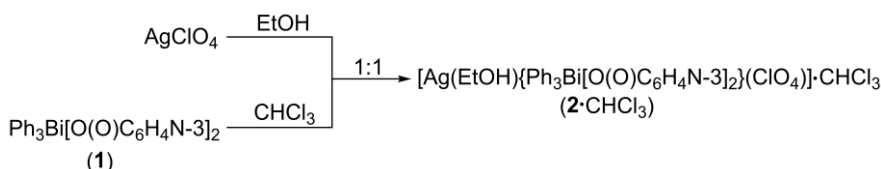
RESULTS

The title compound was obtained when solutions containing equimolar amounts of $\text{Ph}_3\text{Bi}[\text{O}(\text{O})\text{CC}_5\text{H}_4\text{N}-3]_2$ (**1**) in CHCl_3 and AgClO_4 in ethanol (Scheme 1) were layered carefully to avoid their mixing and then the system was left to stand in dark, at room temperature. After several days colorless crystals were isolated, analyzed by IR spectroscopy and the formulation as $[\text{Ag}(\text{EtOH})\{\text{Ph}_3\text{Bi}[\text{O}(\text{O})\text{CC}_5\text{H}_4\text{N}-3]_2\}(\text{ClO}_4)]\cdot\text{CHCl}_3$ (**2** \cdot CHCl_3) was confirmed by single crystal X-ray diffraction studies. The IR spectrum of the title compound,

recorded in KBr pellets, exhibits strong absorption bands in the 1630–1550 and 1380–1340 cm⁻¹ regions, due to stretching vibrations of the carboxyl groups.

Compound **2·CHCl₃** crystallizes in the monoclinic space group **P₁** as a solvate with one molecule of CHCl₃ in the asymmetric unit. A molecule of ethanol, also used as solvent reaction, was found to be included in the coordination sphere

of the silver atom through an Ag···O interaction. This ethanol molecule is disordered over two positions with s.o.f of 0.62(2) and 0.38(2), respectively. The ORTEP-like representation of the molecular structure of **2·CHCl₃** (as fragment of a 1D coordination polymer), with the atom numbering scheme, is depicted in Fig. 1. Selected interatomic distances and bond angles are listed in Table 1.



Scheme 1 – Synthesis of $[\text{Ag}(\text{EtOH})\{\text{Ph}_3\text{Bi}[\text{O}(\text{O})\text{C}_6\text{H}_4\text{N}-3\}_2\}(\text{ClO}_4)]\cdot\text{CHCl}_3$ (**2·CHCl₃**)

Table 1

Selected interatomic distances (Å) and angles (deg) for $[\text{Ag}(\text{EtOH})\{\text{Ph}_3\text{Bi}[\text{O}(\text{O})\text{C}_6\text{H}_4\text{N}-3\}_2\}(\text{ClO}_4)]\cdot\text{CHCl}_3$ (**2·CHCl₃**).^a

Bi(1)–C(13)	2.189(5)		
Bi(1)–C(19)	2.211(5)		
Bi(1)–C(25)	2.195(5)		
Bi(1)–O(1)	2.269(3)	Bi(1)–O(2)	2.269(4)
Bi(1)–O(3a) ⁱ	2.316(3)	Bi(1)–O(4a) ⁱ	2.316(4)
Ag(1)–N(1)	2.196(5)	Ag(1)–O(5)	2.746(6)
Ag(1)–N(2)	2.183(4)	Ag(1)–O(9) [Ag(1)–O(9X)]	2.58(3) [2.60(5)]
C(1)–O(1)	1.291(7)	C(7)–O(3)	1.285(6)
C(1)–O(2)	1.234(7)	C(7)–O(4)	1.223(7)
C(31)–O(9) [C(31X)–O(9X)]	1.34(3) [1.35(5)]	O(9)–H(9) [O(9X)–H(9X)]	0.82 [0.82]
Cl(1)–O(5)	1.413(6)	Cl(1)–O(7)	1.447(6)
Cl(1)–O(6)	1.390(7)	Cl(1)–O(8)	1.392(6)
C(33)–Cl(2)	1.737(8)	C(33)–Cl(4)	1.751(7)
C(33)–Cl(3)	1.698(7)		
O(1)–Bi(1)–O(3a) ⁱ	173.28(13)		
O(1)–Bi(1)–C(13)	88.91(16)	O(3a)–Bi(1)–C(13) ⁱ	94.40(16)
O(1)–Bi(1)–C(19)	86.89(16)	O(3a)–Bi(1)–C(19) ⁱ	86.52(16)
O(1)–Bi(1)–C(25)	89.23(18)	O(3a)–Bi(1)–C(25) ⁱ	91.30(18)
C(13)–Bi(1)–C(19)	108.1(2)	C(19)–Bi(1)–C(25)	106.0(2)
C(13)–Bi(1)–C(25)	145.7(2)		
N(1)–Ag(1)–N(2)	163.06(16)		
N(1)–Ag(1)–O(5)	91.94(17)	N(2)–Ag(1)–O(5)	97.27(17)
N(1)–Ag(1)–O(9) [N(1)–Ag(1)–O(9X)]	92.8(6) [91.5(11)]	N(2)–Ag(1)–O(9) [N(2)–Ag(1)–O(9X)]	101.0(6) [103.9(11)]
O(5)–Ag(1)–O(9) [O(5)–Ag(1)–O(9X)]	92.0(6) [81.3(10)]		
O(1)–C(1)–O(2)	123.5(5)	O(3)–C(7)–O(4)	124.4(4)
O(5)–Cl(1)–O(6)	109.8(4)	O(6)–Cl(1)–O(7)	108.0(4)
O(5)–Cl(1)–O(7)	108.4(3)	O(6)–Cl(1)–O(8)	110.9(4)
O(5)–Cl(1)–O(8)	110.7(4)	O(7)–Cl(1)–O(8)	108.9(4)
Bi(1)–O(1)–C(1)	110.0(3)	Bi(1)–O(3a)–C(7a) ⁱ	105.0(3)
Ag(1)–O(5)–Cl(1)	113.5(3)		

^a Symmetry equivalent atoms: (i) $(x, y, 1+z)$ are given by “a”.

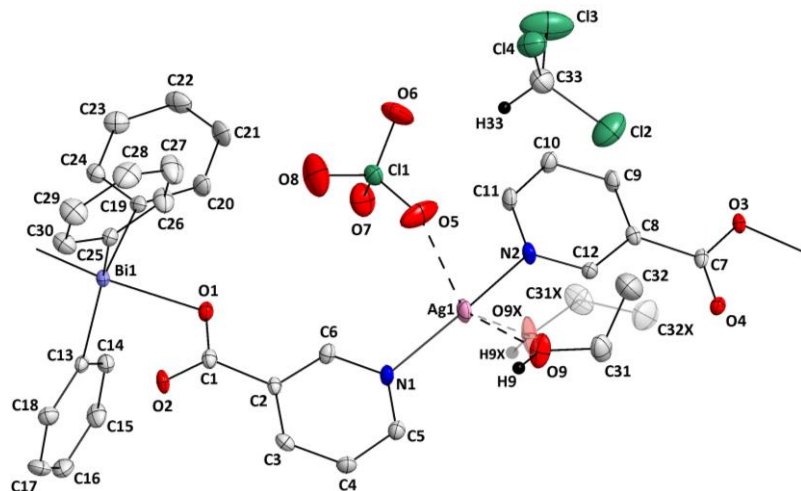


Fig. 1 – Thermal ellipsoid (probability 25%) representation of the molecular structure of **2·CHCl₃**. Hydrogen atoms bonded to carbon atoms, except that of CHCl₃ and EtOH molecules were omitted for clarity. Minor component of the disordered ethanol molecule [atoms labelled with X, s.o.f 0.38(2)] has the transparency set to 0.62.

DISCUSSION

The IR spectrum for **2·CHCl₃**, *i.e.* the higher values than 200 cm⁻¹ for the $\Delta\nu$ between observed asymmetric and symmetric stretching vibrations of the COO group, suggests a monodentate coordination of the carboxylate ligand to the bismuth center. However, intramolecular Bi \cdots O=C contacts are established in solid state as revealed by single-crystal diffraction studies carried out on **2·CHCl₃** (*vide infra*) as well as on both the free metalloligand Ph₃Bi[O(O)CC₅H₄N-3]₂ (**1**) and related silver(I) coordination polymers.¹

The crystal of **2·CHCl₃** contains coordination chain polymers built from triphenylbismuth(V) di(nicotinate) molecules acting as divergent, ditopic metalloligands between silver atoms, with N \rightarrow Ag dative bonds [Ag(1) \cdots N(1) 2.196(5), Ag(1) \cdots N(2) 2.183(4) Å; *cf.* $\Sigma r_{\text{cov}}(\text{Ag}, \text{N})$ 2.16 Å,¹⁶ and $\Sigma r_{\text{vdw}}(\text{Ag}, \text{N})$ 4.25 Å¹⁷] in *trans* to each other [N(1) \cdots Ag(1) \cdots N(2) 163.06(16)°] (Fig. 1). In addition, each silver atom establish rather strong Ag \cdots O interactions with oxygen atoms from an ethanol molecule and a perchlorate anion [Ag(1) \cdots O(9) 2.58(3) Å and Ag(1) \cdots O(5) 2.746(6) Å, respectively; *cf.* $\Sigma r_{\text{cov}}(\text{Ag}, \text{O})$ 2.11 Å,¹⁶ and $\Sigma r_{\text{vdw}}(\text{Ag}, \text{O})$ 4.09 Å¹⁷], both placed almost orthogonal to an imaginary N \cdots Ag \cdots N axis, with an O(5) \cdots Ag(1) \cdots O(9) bond angle of 92.0(6)°. The overall coordination geometry of the resulted AgN₂O₂ core can be described as a distorted *pseudo*-trigonal bipyramidal (“*see-saw*”), as also supported by the value of τ -descriptor (0.68),¹⁸ and the Continuous Shape Measures (CShM) calculations

which indicate a minimal distortion path difference of 2.044 with respect to an ideal “*see-saw*” (SS-4) coordination geometry.¹⁹ Additionally, much weaker Ag(1) \cdots O(7) [3.178(6) Å] and Ag(1) \cdots Cl(7) [3.263(2) Å; *cf.* $\Sigma r_{\text{cov}}(\text{Ag}, \text{Cl})$ 2.47 Å,¹⁶ and $\Sigma r_{\text{vdw}}(\text{Ag}, \text{Cl})$ 4.41 Å¹⁷] interactions are also present.

Natural Bond Orbital (NBO) analysis of the fragment [Ag{O(O)CC₅H₄N-3}₂(ClO₄)(CHCl₃)(EtOH)]²⁻ indicates hypercoordinate interactions around the metal center. Donation takes place mainly from NBOs with lone pair character of nitrogen atoms of the nicotinate ligands in a lone vacant orbital of silver (see Electronic Supplementary information – ESI, Fig. S5). Second order perturbation theory analysis of Fock matrix in NBO basis reveals that the stabilization stemming from N \rightarrow Ag donation is 41.75 and 42.47 kcal/mol, respectively. The electron donation from NBO orbitals of EtOH, ClO₄⁻, or CHCl₃ fragments to silver corresponds to considerably lower energies, which are less than 4 kcal/mol. Natural localized molecular orbitals (NLMO) indicate as well that in Ag–N bonds the largest contributions correspond to the nitrogen atoms (see ESI, Fig. S6).

The Ag–N, Ag \cdots O and Ag \cdots Cl Atoms in Molecules (AIM) bond topologies, the Non-Covalent Interaction (NCI) and Interaction Region Indicator (IRI) iso-surfaces and their plots *vs* sign($\lambda_2\rho$) corresponding to [Ag{O(O)CC₅H₄N-3}₂(ClO₄)(CHCl₃)(EtOH)]²⁻ fragment are presented in ESI, Figs. S9 and S11–S14, respectively.

Quantum Theory of Atoms in Molecules (QTAIM) descriptors of both Ag–N bonds as well as the Ag \cdots O interaction with the ethanol molecule are similar (see ESI, Table S3). The small values of

$\rho(r)$ and the positive values of $\nabla^2\rho(r)$ suggest the interactions between the silver atom and the donor atoms are closed shell interactions, aspect confirmed also by the values of $|V(r)|/G(r)$ ratio which are < 1 .²⁰ Strong polar character of the bonds is also indicated by the $G(r)/\rho(r)$ ratio coupled to small negative values for $H(r)$. By contrast, the $\text{Ag}\cdots\text{O}$ interactions with the perchlorate anion, as well as $\text{Ag}\cdots\text{Cl}$ contacts have even smaller values for $\rho(r)$ and small positive $\nabla^2\rho(r)$. Small positive values of $H(r)$, $G(r)/\rho(r)$ ratio > 1 and $1 < |V(r)|/G(r) < 2$ for the later indicate more a dispersive nature of these bonds.^{20,21} The Intrinsic Bond Strength Indexes (IBSI) (see ESI, Table S1) reveal a slightly different bonding picture around the metal,²² indicating that only $\text{Ag}\cdots\text{N}$ bonds are at the borderline to coordinate bond whereas the $\text{Ag}\cdots\text{O}$ and $\text{Ag}\cdots\text{Cl}$ interactions correspond to non-covalent interactions. However, the IBSI values for $\text{Ag}\cdots\text{O}_{\text{ethanol}}$ and one $\text{Ag}\cdots\text{O}_{\text{perchlorate}}$ interactions are more than double the other two and support thus the above selected coordination geometry around the metal center. This observation is consistent with iso-surfaces obtained with the Reduced Density Gradient (RDG) method and Interaction Region Indicator (IRI).²³

The coordination geometry around the bismuth atom of the metalloligand in **2**·CHCl₃ is distorted trigonal bipyramidal with the oxygen atoms of the carboxylate groups in apical positions. The O–Bi–O bond angle [O(1)–Bi(1)–O(3a) 173.28(13)°] as well as the Bi–O bond lengths [Bi(1)–O(1) 2.269(3) Å; Bi(1)–O(3a) 2.316(3) Å] in the polymeric chain of **2**·CHCl₃ are in the range reported for the structures of related molecular Ph₃Bi[O(O)CR]₂ carboxylates included in Cambridge Structure Database²⁴ [*e.g.* O–Bi–O angles from 167.0(1)° in Ph₃Bi[O(O)CC₆H₃(OH)-2-Br-5]₂·Et₂O,²⁵ to 176.3(1)° in Ph₃Bi[O(O)CCH(OH)Ph-(R)]₂,²⁶ Bi–O bond lengths from 2.247(4) Å in Ph₃Bi[O(O)CC₆H₃Cl₂-3,5]₂,²⁷ or 2.247(3) Ph₃Bi[O(O)CC₆H₄(OH)-2]₂,²⁸ to 2.386(6) Å in Ph₃Bi[O(O)CC₆H₃F₂-2,3]²⁹] and close to the values reported by us for free Ph₃Bi[O(O)CC₅H₄N-3]₂ [O–Bi–O 172.32(11)°; Bi–O 2.299(3), 2.303(3) Å] and its silver(I) complexes, *i.e.* [Ag{Ph₃Bi[O(O)CC₅H₄N-3]₂}](OTf)·CH₂Cl₂ [O–Bi–O 172.7(3), 172.8(3)°; Bi–O 2.278(7), 2.283(7); 2.274(7), 2.303(7) Å, for the two independent molecules in the crystal], [Ag{Ph₃Bi[O(O)CC₅H₄N-3]₂}](SbF₆)·CH₂Cl₂ [O–Bi–O 173.8(2)°; Bi–O 2.306(5), 2.320(5) Å], or [Ag{Ph₃Bi[O(O)CC₅H₄N-3]₂}](NO₃)·CH₂Cl₂ [O–Bi–O 174.5(3)°; Bi–O 2.295(7), 2.314(7) Å].¹ The description of the coordination geometry around

the bismuth atom in **2**·CHCl₃ as distorted trigonal bipyramidal is consistent with CShM calculations which indicate a minimal distortion path difference of 1.274 with respect to an ideal trigonal bipyramidal (TBPY-5).³⁰ However, by contrast, the value of τ-descriptor (0.46) indicates a geometry somewhat closer to a square pyramid (SPY-5) than a TBPY-5.³¹

In addition, within a metalloligand unit in **2**·CHCl₃ the bismuth-oxygen distances [Bi(1)–O(2) 2.852(3) Å; Bi(1)–O(4a) 2.961(4) Å] between the metal and the doubly bonded oxygen atom of a carboxylate group are similar to the analogous distances [Bi–O(=C) 2.840(3), 2.860(4) Å] in the free molecule of Ph₃Bi[O(O)CC₅H₄N-3]₂,¹ they are in the range of the related distances reported for other triphenylbismuth(V) dicarboxylates [*e.g.* Bi–O(=C) distances from 2.653(5) in Ph₃Bi[O(O)CC₆H₂(OMe)₃-3,4,5]₂,²⁷ to 3.176(9) in Ph₃Bi{O(O)CC₆F₅}₂,³²] and well shorter than the sum of van der Waals radii for the corresponding atoms [*cf.* $\Sigma r_{\text{cov}}(\text{Bi}, \text{O})$ 2.14 Å,¹⁶ and $\Sigma r_{\text{vdw}}(\text{Bi}, \text{O})$ 4.04 Å¹⁷].

Second order perturbation theory analysis of Fock matrix in NBO basis indicates that in the metalloligand the Bi–O bonds are based on donation of electron density (largest contributions to the stabilization energy are 76.91, 12.67, 65.63 and 11.59 kcal/mol) from NBO orbitals with lone pair character on the oxygen atoms in an empty, with mainly *p* character, orbital of bismuth (see ESI, Fig. S7). This suggests a 4*e*-3*c* bonding pattern between Ph₃Bi fragment and the two nicotinate ligands. Stabilization by donation from the electron pairs of the oxygen atom of the C=O group in empty orbitals of bismuth have considerably smaller values (< 4 kcal/mol) than those corresponding to Bi–O bonds. The large values of the oxygen atoms contributions in Natural Localized Molecular Orbitals (NLMOs) of Ph₃Bi[O(O)CC₅H₄N-3]₂ indicate a significant polarization of the Bi–O bonds (see ESI, Fig. S8), in contrast to NLMOs of Bi–C bonds which have comparable values in atomic contributions of the atomic orbitals of the elements.

Bond topologies, the NCI and IRI iso-surfaces and their plots *vs* sign($\lambda_2\rho$) corresponding to metalloligand Ph₃Bi[O(O)CC₅H₄N-3]₂ are shown in ESI, Fig. S10 and Figs. S15–S18. Surprisingly, in the QTAIM framework, no bond critical points (BCP) were obtained between the oxygen atoms of the C=O groups and the bismuth atom. The descriptors of BCP of Bi–C and Bi–O bonds are included in ESI, Table S6.

The values of the $\rho(r)$, $\nabla^2\rho(r)$ and negative values of $H(r)$ corresponding to Bi–C and Bi–O

bonds are consistent to those reported for typical donor-acceptor, closed shell interactions found in complexes.³³ However, only Bi–O have $G(r)/\rho(r)$ values close to 1, as reported for transition metal complexes not also the Bi–C bonds.

In $\text{Ph}_3\text{Bi}[\text{O}(\text{O})\text{CC}_5\text{H}_4\text{N}-3]_2$, although there is missing a BCP, the IBSI of $\text{Bi}\cdots\text{O}(=\text{C})$ interactions have a small value (see ESI, Table S2), several orders in magnitude less than Bi–C or Bi–O bonds, but in the range of the values found for the non-covalent interactions.²² This value is consistent with aspect of the surfaces green areas of the surfaces located between Bi and O(=C) atoms obtained using the RDG method and interaction region indicator (IRI).²³

In the coordination polymer **2**· CHCl_3 , like in all the other structures of $\text{Ph}_3\text{Bi}[\text{O}(\text{O})\text{CR}]_2$ species, the largest C–Bi–C angle [C(13)–Bi(1)–C(25) 145.7(2) $^\circ$] of the metalloligand moiety encloses the polyhedron edge that contains the doubly bonded oxygen atoms of the carboxylate groups. This C–Bi–C bond angle is in the range of analogous reported values for other related structures [*i.e.* C–Bi–C from 133.5(1) $^\circ$ $\text{Ph}_3\text{Bi}[\text{O}(\text{O})\text{CB}_{10}\text{H}_{10}\text{C}_2\text{-1,2-Me-2-closo}]_2$,³⁴ to 157.1(2) $^\circ$ $\text{Ph}_3\text{Bi}[\text{O}(\text{O})\text{C-1-adamantyl}]_2$,³⁵], and close to the value reported for $\text{Ph}_3\text{Bi}[\text{O}(\text{O})\text{CC}_5\text{H}_4\text{N}-3]_2$ [140.9(2) $^\circ$.¹ The torsion angle defined by the oxygen atoms of the carboxylate groups [−4.3(2) $^\circ$] indicates a *syn*-periplanar conformation in the metalloligand unit.

The angle between the best planes of the heterocycles from a metalloligand unit in the

coordination polymer **2**· CHCl_3 is 10.0(2) $^\circ$. The nitrogen atoms are in position *trans* with respect to the plane perpendicular on the heterocycles, situation similar to that observed for the free $\text{Ph}_3\text{Bi}\{\text{O}(\text{O})\text{CC}_5\text{H}_4\text{N}-3\}_2$ and its previously reported silver(I) complexes.¹ This arrangement affords the triphenylbismuth(V) dicarboxylate to act as *exo*-bidentate spacer in this coordination polymer, with a N(1)–N(1a) distance of 12.664(7) Å within a metalloligand unit.

In the crystal of **2**· CHCl_3 several different types of intermolecular interactions at distances shorter than the sum of the van der Waals radii of the corresponding atoms are established between parallel chains of the coordination polymers (Fig. 2). The chain polymer with alternating silver(I) atoms and organobismuth(V) metalloligands is supported by additional C–H···O [C(33)–H(33)_{chloroform}···O(6)_{perchlorate} 2.242(6) Å and C(26)–H(26)_{phenyl}···O(8)_{perchlorate} 2.610(6) Å; *cf.* the sum of the van der Waals radii of the corresponding atoms, $\Sigma r_{\text{vdW}}(\text{O}, \text{H})$ 2.70 Å¹⁷] and C–H···Cl [C(32)–H(32B)_{ethanol}···Cl(2)_{chloroform} 2.785(3) Å; *cf.* the sum of the van der Waals radii of the corresponding atoms, $\Sigma r_{\text{vdW}}(\text{Cl}, \text{H})$ 3.02 Å¹⁷] as well as C–Cl···π (Py_{centroid}) interactions [C(33)–Cl(2)_{chloroform}···Py_{centroid}{C(8)–C(11), N(2), C(12)} 3.659(2) Å, $\gamma = 2.9^\circ$ (angle between the normal to the pyridyl ring and the line defined by the Cl atom and Py_{centroid}] (Fig. 2).

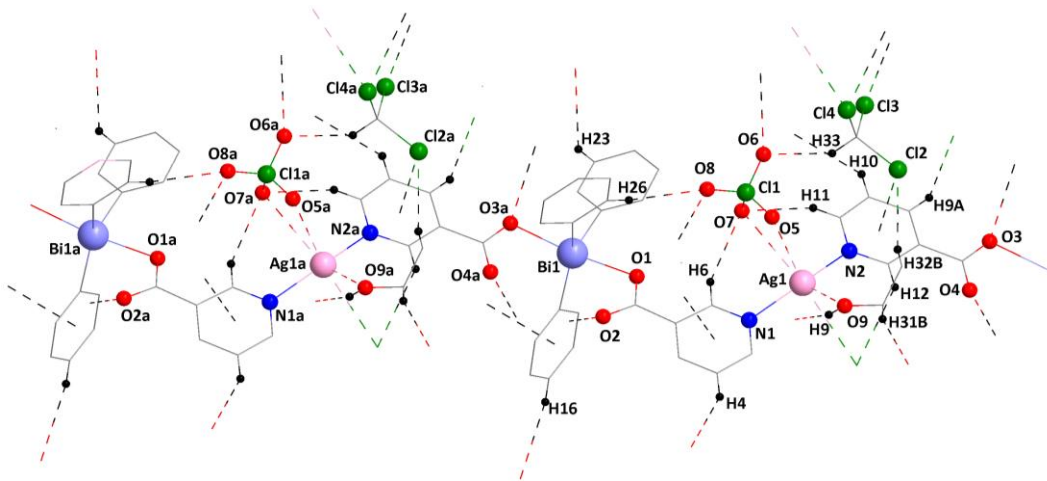


Fig. 2 – Fragment of 1D coordination polymer in the crystal of **2**· CHCl_3 , showing all types of interchain interactions including those established by perchlorate anions (*i.e.* $\text{Ag}\cdots\text{O}$ and $\text{C-H}\cdots\text{O}$) and solvent molecules [*i.e.* $\text{Ag}\cdots\text{O}$, $\text{O-H}\cdots\text{O}$, $\text{C-H}\cdots\text{O}$ and $\text{C-H}\cdots\text{Cl}$ for ethanol, and $\text{Ag}\cdots\text{Cl}$, $\text{C-H}\cdots\text{Cl}$ and $\text{Cl}\cdots\pi$ for chloroform] as well as $\text{C-H}\cdots\pi$ and $\pi\cdots\pi$ interactions [symmetry equivalent atoms (x, y, z), ($-1+x, y, 1+z$), ($2-x, 1-y, 1-z$), ($1-x, -y, 1-z$), ($1-x, -y, -z$), ($1+x, y, z$), ($2-x, 1-y, -z$) and ($1-x, 1-y, 1-z$) are given by “a”, “t”, “u”, “v”, “w”, “x”, “y” and “z”].

Layers are built from parallel chains connected through $\text{C-H}\cdots\text{O}$ interactions [C(16t)–H(16t)_{phenyl}···O(3)_{carboxylate} 2.661(7) Å] and bridging chloroform

solvent molecules [in addition to the above mentioned interactions supporting the chain polymer, other $\text{Ag}(1x)\cdots\text{Cl}(4)\text{chloroform}$ 3.263(2) Å and $\text{C}(12x)$

$\text{H}(12\text{x})_{\text{pyridyl}} \cdots \text{Cl}(4)$ 2.886(2) Å interactions are established with the neighboring chain polymer] (see Figs. S2–S4, in the Electronic Supplementary information – ESI). An extended 3D architecture is built in the crystal of **2**· CHCl_3 from parallel layers connected by bridging ethanol molecules [involving moderate hydrogen bonding, $\text{O}(9)-\text{H}(9)_{\text{ethanol}} \cdots \text{O}(2\text{v})_{\text{carboxylate}}$ 2.088(4) Å, and weak C–H \cdots O interactions, $\text{C}(31)-\text{H}(31\text{B})_{\text{ethanol}} \cdots \text{O}(4\text{w})_{\text{carboxylate}}$ 2.640(4) Å], chloroform molecules [$\text{C}(9\text{y})-\text{H}(9\text{y})_{\text{pyridyl}} \cdots \text{Cl}(3)_{\text{chloroform}}$ 2.881(3) Å] and perchlorate anions [weak C–H \cdots O interactions: $\text{C}(23\text{t})-$

$\text{H}(23\text{t})_{\text{phenyl}} \cdots \text{O}(6)_{\text{perchlorate}}$ 2.661(7) Å, $\text{C}(4\text{v})-\text{H}(4\text{v})_{\text{pyridyl}} \cdots \text{O}(8)_{\text{perchlorate}}$ 2.650(7) Å]. Additional inter-layers C–H $\cdots\pi$ ($\text{Ph}_{\text{centroid}}$) interactions [$\text{C}(10)-\text{H}(10)_{\text{pyridyl}} \cdots \text{Ph}_{\text{centroid}}\{\text{H}13\text{z}-\text{H}18\text{z}\}$ 2.832(1) Å, $\gamma = 3.8^\circ$; cf. H $\cdots\text{Ar}_{\text{centroid}}$ contacts shorter than 3.1 Å and an angle γ between the normal to the aromatic ring and the line defined by the H atom and $\text{Ar}_{\text{centroid}}$ smaller than 30° ,³⁶ as well as π ($\text{Py}_{\text{centroid}}$) $\cdots\pi$ ($\text{Py}_{\text{centroid}}$) interactions between parallel rings [$\text{Py}_{\text{centroid}}\{\text{C}(2)-\text{C}(5),\text{N}(1),\text{C}(6)\} \cdots \text{Py}_{\text{centroid}}\{\text{C}(2\text{y})-\text{C}(5\text{y}),\text{N}(1\text{y}),\text{C}(6\text{y})\}$ 3.634(1) Å] are also present (Fig. 3).

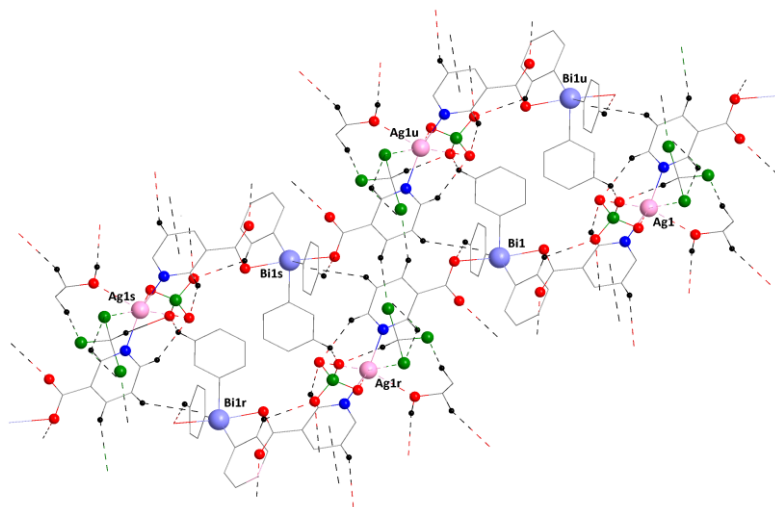


Fig. 3 – Fragment of the 3D structure built through non-covalent interactions between coordination polymers in the crystal of **2**· CHCl_3 [symmetry equivalent atoms ($x, y, 1+z$), ($2-x, 1-y, 2-z$) and ($2-x, 1-y, 1-z$) are given by “r”, “s” and “u”].

The normalized contact distance (d_{norm}) mapped on the Hirschfeld surface of **2**· CHCl_3 indicates that most of distances shorter than sum of van der Waals radii (represented with red) are consistent to those previously described (see ESI, Figs. S19–S20).³⁷ The 2D fingerprint plots of d_e and d_i functions indicates that in the crystal architecture (see ESI, Fig. S21) the most numerous intermolecular close contracts correspond to H \cdots H, C \cdots H, and O \cdots H. The N \cdots H, Ag \cdots O, and Ag \cdots Cl and other interatomic contacts contribute with less than 10% to the Hirshfeld surface.

EXPERIMENTAL

The metalloligand $\text{Ph}_3\text{Bi}[\text{O}(\text{O})\text{CC}_5\text{H}_4\text{N}-3]_2$ (**1**) was prepared according to a literature procedure.¹ The infrared spectrum was recorded as KBr pellets in the 4000–600 cm⁻¹ range on a Bruker Vector 22 spectrometer. ESI mass spectra were recorded on a Thermo Scientific Orbitrap XL spectrometer equipped with standard source. Data analysis and calculations of the theoretical isotopic patterns were carried out with the Xcalibur software package.³⁸

Synthesis of $\text{Ag}(\text{EtOH})\{\text{Ph}_3\text{Bi}[\text{O}(\text{O})\text{CC}_5\text{H}_4\text{N}-3]_2\}(\text{ClO}_4)\cdot\text{CHCl}_3$ (2· CHCl_3)

A solution of AgClO_4 (10 mg, 48 mmol) in EtOH (5 mL) in absence of light was layered on a solution of $\text{Ph}_3\text{Bi}[\text{O}(\text{O})\text{CC}_5\text{H}_4\text{N}-3]_2$ (33 mg, 48 mmol) in CHCl_3 (10 mL). The reaction mixture was kept at room temperature and colorless crystals of the title compound, suitable for single crystal X-ray diffraction analysis, deposited after two weeks and were collected by filtration. IR (KBr pellet, $\tilde{\nu}$, cm⁻¹): 3074 (vw), 2958 (s), 2924 (vs), 2852 (s), 1626 (s), 1597 (m) [$\text{v}_{\text{as}}(\text{COO})$], 1558 (w), 1469 (m), 1436 (m), 1373 (s), 1345 (vs) [$\text{v}_s(\text{COO})$], 1315 (m), 1196 (w), 1149 (vw), 984 (w), 857 (w), 759 (m), 733 (s), 676 (m). MS (ESI+, MeCN): m/z 106.90 ([Ag^+], 8), 147.93 ([$\text{Ag} + \text{MeCN}$]⁺, 24), 188.96 ([$\text{Ag} + 2\text{MeCN}$]⁺, 10), 208.98 ([Bi^+], 34), 229.94 ([$\text{Ag} + \text{HO}(\text{O})\text{CC}_5\text{H}_4\text{N}-3$]⁺, 2), 270.96 ([$\text{Ag} + \text{HO}(\text{O})\text{CC}_5\text{H}_4\text{N}-3 + \text{MeCN}$]⁺, 1), 286.02 ([[PhBi]^+], 4), 363.06 ([$\text{[Ph}_2\text{Bi}^+$], 10), 457.10 ([$\text{[Ph}_3\text{Bi} + \text{OH}]^+$], 2), 471.12 ([$\text{[Ph}_3\text{Bi} + \text{OMe}]^+$], 12), 517.14 ([$\text{[Ph}_4\text{Bi}]^+$], 100), 545.13 ([$\text{[Ph}_4\text{Bi} + \text{CO}]^+$], 4). MS (ESI+, MeOH): m/z 124.04 ([$\text{[HO}(\text{O})\text{CC}_5\text{H}_4\text{N}-3 + \text{H}]^+$], 4), 208.98 ([[Bi^+], 34), 286.02 ([$\text{[PhBi}]^+$], 26), 363.06 ([$\text{[Ph}_2\text{Bi}^+$], 18), 457.10 ([$\text{[Ph}_3\text{Bi} + \text{OH}]^+$], 100), 471.12 ([$\text{[Ph}_3\text{Bi} + \text{OMe}]^+$], 76), 499.11 ([$\text{[Bi} + \text{O}(\text{O})\text{CMe}]^+$], 24), 517.14 ([$\text{[Ph}_4\text{Bi}]^+$], 4), 562 ([$\text{[Ph}_3\text{Bi} + \text{O}(\text{O})\text{CC}_5\text{H}_4\text{N}-3]$]⁺, 42). MS (ESI-, MeOH): m/z 98.95 ([[ClO_4^-], 5), 122.03 ([$\text{[O}(\text{O})\text{CC}_5\text{H}_4\text{N}-3]$]⁻, 100), 267.04 ([$\text{[2O}(\text{O})\text{CC}_5\text{H}_4\text{N}-3 + \text{Na}]^-$, 84). HRMS (ESI+, MeOH): m/z

[Ph₃Bi + O(O)CC₅H₄N-3]⁺ calcd for C₂₄H₁₉BiNO₂, 562.12079; found, 562.12141.

Crystal structure determination

Crystallographic data for **2**·CHCl₃ were collected at 200 K on a Rigaku Oxford-Diffraction Xcalibur E CCD diffractometer, with graphite monochromator, using MoK α radiation (0.71073 Å). The structures were solved with SHELXT 2015,³⁹ and refined with the SHELX-2018 using Olex2 as graphical interface.^{40,41} All the non-hydrogen atoms were treated anisotropically. Hydrogen atoms were included in riding positions with the isotropic thermal parameters set 1.2 times the thermal parameters of the carbon atoms directly attached for the aromatic hydrogen atoms and 1.5 times for the methyl and the hydroxyl group hydrogen atoms, respectively. Further details on the data collection and refinement methods can be found in Table 2. The

ethanol molecule coordinated to the silver atom is disordered over two positions with s.o.f of 0.62(2) and 0.38(2), respectively. The C–C bond length of the two components of the disorder were restrained to be equal. Also, the U_{ij} were restrained to be equal for oxygen and the carbon atoms in each component of the disorder. The reflections with the hkl indices 0 1 0 and 1 0 1, likely affected by the beam stop, were omitted from the refinement. Continuous shape measures (CShM's) of the coordination polyhedral were calculated with the software SHAPE.⁴² The position of the ring centroid and intra- and intermolecular interactions were evaluated with PLATON software package.⁴³ The representations of the molecular structure and those describing the supramolecular architectures were carried out using Diamond.⁴⁴ Analysis of the intermolecular interactions was performed with CrystalExplorer.⁴⁵ Van der Waals radii used in the analysis were those reported by Alvarez.¹⁷

Table 2

Crystallographic data for [Ag(EtOH){Ph₃Bi[O(O)CC₅H₄N-3]₂}({ClO₄)·CHCl₃ (**2**·CHCl₃)}

Empirical formula	C ₃₃ H ₃₀ AgBiCl ₄ N ₂ O ₉
Formula weight	1057.24
Crystal size /mm	0.15 × 0.20 × 0.25
Crystal habit	clear light colorless prism
Wavelength MoK α (Å)	0.71073
Temperature (K)	200
Crystal system	triclinic
Space group	<i>P</i> ̄1 (No. 2)
<i>a</i> (Å)	8.8572(4)
<i>b</i> (Å)	13.5455(5)
<i>c</i> (Å)	15.5985(6)
α (°)	85.564(3)
β (°)	84.737(3)
γ (°)	84.668(3)
Volume (Å ³)	1851.02(13)
<i>Z</i>	2
Density (calculated) (g cm ⁻³)	1.897
Absorption coefficient μ (MoK α) (mm ⁻¹)	5.619
<i>F</i> (000)	1024
θ range for data collections (°)	1.93 – 25.03
<i>T</i> _{max} / <i>T</i> _{min}	0.987 / 1.000
Reflections collected	15035
Independent reflections, <i>R</i> _{int}	6543, 0.0432
Miller indices, <i>h</i> , <i>k</i> , <i>l</i> (min/max)	-10/8, -16/16, -18/17
Refinement method	Full-matrix least-squares on F ²
Data / restraints / parameters	6543 / 25 / 481
Goodness-of-fit on F ²	1.037
Final <i>R</i> indices [<i>I</i> > 2σ(<i>I</i>)]	<i>R</i> ₁ = 0.0364 <i>wR</i> ₂ = 0.0698
<i>R</i> indices (all data)	<i>R</i> ₁ = 0.0429 <i>wR</i> ₂ = 0.0723
Largest diff. peak and hole, eÅ ⁻³	-0.81, 1.12

Theoretical calculations

Theoretical calculations were carried out on the molecular structure fragments Ph₃Bi[O(O)CC₅H₄N-3]₂ and [Ag{O(O)CC₅H₄N-3}₂(ClO₄)(CHCl₃)]²⁻. For calculation

only the major component of the disordered ethanol molecule was considered. The position of the hydrogen atoms was optimized using ORCA 5.0.3 software package.⁴⁶ The coordinates of the non-hydrogen atoms were maintained those found in the molecular structure determined by single-crystal X-ray diffraction. Calculations were carried out using PBE functional,⁴⁷ in conjunction with def2-TZVPP basis set,⁴⁸ the

corresponding auxiliary basis set for the RI approximation,⁴⁹ and the atom-pairwise dispersion correction with the Becke-Johnson damping scheme (D3BJ).⁵⁰ For silver and bismuth the 28 and 46, respectively, core electrons were replaced with ECPs.^{51,52}

Single point calculations on the geometries obtained with ORCA were carried out with Gaussian 09, Revision E.01,⁵³ using the PBE functional,⁴⁷ and the def2-TZVPP basis set.⁴⁸ The dispersion corrections were accounted for using the D3 version of Grimme's dispersion with Becke-Johnson damping.^{50b}

The natural bond orbital analyses were carried out with NBO 7.0.5,⁵⁴ atoms in molecules with AIMall 19.10.12,⁵⁵ and NCI with Multiwfn 3.8, respectively.⁵⁶

CONCLUSIONS

A new heterometallic silver(I) complex was obtained by reacting AgClO_4 with $\text{Ph}_3\text{Bi}[\text{O}(\text{O})\text{CC}_5\text{H}_4\text{N}-3]_2$ in CHCl_3 /ethanol solvent mixture, *i.e.* $[\text{Ag}(\text{EtOH})\{\text{Ph}_3\text{Bi}[\text{O}(\text{O})\text{CC}_5\text{H}_4\text{N}-3]\}_2](\text{ClO}_4)\cdot\text{CHCl}_3$. The investigation of the solid state structure by means of single-crystal X-ray diffraction revealed the formation of a chain coordination polymer in which Ag(I) cations are bridged by divergent, ditopic organometallic ligand moieties through $\text{Ag}\cdots\text{N}_{\text{nicotinate}}$ bonds. The coordination number of the silver atom in the linear $\text{N}\text{--Ag}\text{--N}$ core is increased by additional $\text{Ag}\cdots\text{O}_{\text{perchlorate}}$ and $\text{Ag}\cdots\text{O}_{\text{ethanol}}$ interactions. A 3D architecture is built in the crystal of this heterometallic silver(I)/bismuth(V) complex based on non-covalent $\text{O}\text{--H}\cdots\text{O}$, $\text{C}\text{--H}\cdots\text{O}$, $\text{C}\text{--H}\cdots\text{Cl}$, $\text{Ag}\cdots\text{Cl}$ as well as $\text{C}\text{--H}\cdots\pi$ ($\text{Ph}_{\text{centroid}}$) and $\pi\cdots\pi$ ($\text{Py}_{\text{centroid}}$) interactions.

Supplementary material. The CCDC reference number for **2** $\cdot\text{CHCl}_3$ is 2235286. The supplementary crystallographic data can be obtained free of charge from The Cambridge Crystallographic Data Centre via <https://www.ccdc.cam.ac.uk/structures/>.

Acknowledgements. This work was supported by a grant of Ministry of Research and Innovation, CNCS – UEFISCDI, project number PN-III-P4-ID-PCCF-2016-0088. The support provided by CSI Dr. Sergiu SHOVA (“Petru Poni” Institute of Macromolecular Chemistry, 41A Aleea Grigore Ghica Vodă, 700487 Iași, Roumania) for XRD determination and refinement is highly acknowledged.

REFERENCES

1. A. B. Kiran, T. Mocanu, A. Pöllnitz, S. Shova, M. Andruh and C. Silvestru, *Dalton Trans.*, **2018**, *47*, 2531–2542, and references cited therein.
2. See selected references for ferrocenene carboxylate complexes: (a) X.-M. Cai, T. K. Meister, A. Pöthig and F. E. Kühn, *Inorg. Chem.*, **2016**, *55*, 858–864, and references therein; (b) B. Y. Chor, R. Ganguly and W. K. Leong, *J. Organomet. Chem.*, **2016**, *802*, 15–20; (c) Y. Fan, H.-M. Li, R.-H. Duan, H.-T. Lu, J.-T. Cao, G.-D. Zou and Q.-S. Jing, *Inorg. Chem.*, **2017**, *56*, 12775–12782; (d) S. Li, X.-S. Du, B. Li, J.-Y. Wang, G.-P. Li, G.-G. Gao and S.-Q. Zang, *J. Am. Chem. Soc.*, **2018**, *140*, 2, 594–597; (e) N. Johns, S. M. Balasekaran, A. Chang, P. K. Bhowmik and F. Poineau, *Inorg. Chim. Acta*, **2019**, *489*, 115–119; (f) P. S. Koroteev, Z. V. Dobrokhotova, A. B. Ilyukhin, E. V. Belova, A. D. Yaprutsev, M. Rouzières, R. Clérac and N. N. Efimov, *Dalton Trans.*, **2021**, *50*, 16990–16999; (g) V. V. Sharutin and O. K. Sharutina, *Russ. J. Coord. Chem.*, **2022**, *48*, 173–179; (h) I. A. Yakushev, M. A. Dyuzheva, I. A. Stebletsova, A. B. Kornev, N. V. Cherkashina and M. N. Vargaftik, *Russ. J. Coord. Chem.*, **2022**, *48*, 153–163; (i) E.-M. Han, W.-D. Yu, B. Wang, J. Yan, X.-Y. Yi and C. Liu, *Inorg. Chem.*, **2022**, *61*, 2903–2910.
3. See selected references for 1,1'-ferrocenene carboxylate complexes: (a) R. Singh and P. K. Bharadwaj, *Cryst. Growth Des.*, **2013**, *13*, 3722–3733; (b) Z. Liu, J. Lei, M. Frasconi, X. Li, D. Cao, Z. Zhu, S. T. Schnabeli, G. C. Schatz and J. F. Stoddart, *Angew. Chem. Int. Ed.*, **2014**, *53*, 9193–9197; (c) M. L. Ospina-Castro, A. Reiber, G. Jorge, E. E. Ávila and A. Briceño, *CrystEngComm*, **2017**, *19*, 758–761; (d) R. Jambor, Z. Růžičková, M. Erben and L. Dostál, *Inorg. Chem. Commun.*, **2017**, *76*, 36–39; (e) X.-D. Du, W. Zheng, X.-H. Yi, J.-P. Zhao, P. Wang and C.-C. Wang, *CrystEngComm*, **2018**, *20*, 2608–2616; (f) Q. Miao, F. Rouhani, H. Moghanni-Bavil-Olyaei, K.-G. Liu, X.-M. Gao, J.-Z. Li, X.-D. Hu, Z.-M. Jin, M.-L. Hu and A. Morsali, *Chem.-Eur. J.*, **2020**, *26*, 9518–9526; (g) J. Benecke, E. S. Grape, T. A. Engesser, A. Ken Inge and H. Reinsch, *CrystEngComm*, **2020**, *22*, 5569–5572; (h) M. L. Ospina-Castro, E. E. Avila, A. Briceno, A. Reiber, L. C. Pacheco-Londono and N. J. Galan-Freyle, *CrystEngComm*, **2021**, *23*, 8198–8208; (i) E.-M. Han, W.-D. Yu, L.-J. Li, X.-Y. Yi, J. Yan and C. Liu, *Chem. Commun.*, **2021**, *57*, 2792–2795; (j) R. Gao, S.-M. Chen, F. Wang and J. Zhang, *Inorg. Chem.*, **2021**, *60*, 239–245; (k) J. Benecke, A. Fu, T. A. Engesser, N. Stock and H. Reinsch, *Eur. J. Inorg. Chem.*, **2021**, 713–719; (l) S.-J. Yao, N. Li, J. Liu, L.-Z. Dong, J.-J. Liu, Z.-F. Xin, D.-S. Li, S.-L. Li and Y.-Q. Lan, *Inorg. Chem.*, **2022**, *61*, 2167–2173.
4. See, for example, selected references: (a) C. Gwengo, R. Iyer and M. Raja, *Cryst. Growth Des.*, **2012**, *12*, 49–53; (b) M. Raja, R. G. Iyer, C. Gwengo, D. L. Reger, P. J. Pellechia, M. D. Smith and A. E. Pascui, *Organometallics*, **2013**, *32*, 95–103; (c) T. Miyazaki, H. Tanaka, Y. Tanabe, M. Yuki, K. Nakajima, K. Yoshizawa and Y. Nishibayashi, *Angew. Chem., Int. Ed.*, **2014**, *53*, 11488–11492; (d) B. E. Cowie, F. A. Tsao and D. J. H. Emslie, *Angew. Chem., Int. Ed.*, **2015**, *54*, 2165–2169; (e) S. Handa, E. D. Slack and B. H. Lipshutz, *Angew. Chem., Int. Ed.*, **2015**, *54*, 11994–11998; (f) L. M. Guard, M. M. Beromí, G. W. Brudvig, N. Hazari and D. J. Vinyard, *Angew. Chem., Int. Ed.*, **2015**, *54*, 13352–13356; (g) T. He, H. Wu, X. Wang, Q. Zang, P. Xue, R. Shen, L. Dang, Y. Zhang and J. Xiang, *Cryst. Growth Des.*, **2016**, *16*, 6239–6249; (h) V. Croué, S. Goeb, G. Szaloki, M. Allain and M. Salle, *Angew. Chem., Int. Ed.*, **2016**, *55*, 1746–1750; (i) B. Deka, T. Sarkar, S. Banerjee, A. Kumar, S. Mukherjee, S. Deka, K. K. Saikia and A. Hussain, *Dalton Trans.*, **2017**, *46*, 396–409; (j) W. L. Huang and P. L. Diaconescu, *Organometallics*, **2017**, *36*, 89–96; (k) J. Oetzel, N. Weyer, C. Bruhn, M. Leibold, B. Gerke, R. Pöttgen, M. Maier, R. F. Winter, M. C. Holthausen and U. Siemeling, *Chem.-Eur. J.*, **2017**, *23*, 1187–1199; (l) J. Mahrholdt,

- T. Rüffer and H. Lang, *Z. Anorg. Allg. Chem.*, **2020**, *646*, 1634–1640; (m) M. Allison, P. Carames-Mendez, C. M. Pask, R. M. Phillips, R. M. Lord and P. C. McGowan, *Chem.-Eur. J.*, **2021**, *27*, 3737–3744; (n) S. Gadre, M. Manikandan, P. Duari, S. Chhatar, A. Sharma, S. Khatri, J. Kode, M. Barkume, N. K. Kasinathan, M. Nagare, M. Patkar, A. Ingle, M. Kumar, U. Kolthur-Seetharam and M. Patra, *Chem.-Eur. J.*, **2022**, *28*, e202201259; (o) D. Yamamoto, I. Hirano, Y. Narushima, M. Soga, H. Ansai and K. Makino, *Green Chem.*, **2022**, *24*, 7162–7170.
5. (a) M. Oh, G. B. Carpenter and D. A. Sweigart, *Acc. Chem. Res.*, **2004**, *37*, 1–11, and references therein; (b) M. Oh, J. A. Reingold, G. B. Carpenter and D. A. Sweigart, *Coord. Chem. Rev.*, **2004**, *248*, 561–569, and references therein; (c) J. A. Reingold, M. Z. Jin and D. A. Sweigart, *Inorg. Chim. Acta*, **2006**, *359*, 1983–1987.
6. (a) J. Moussa, K. M.-C. Wong, L.-M. Chamoreau, H. Amouri and V. W.-W. Yam, *Dalton Trans.*, **2007**, 3526–3530; (b) J. Moussa and H. Amouri, *Angew. Chem., Int. Ed.*, **2008**, *47*, 1372–1380, and references therein; (c) J. Moussa, K. M.-C. Wong, X. F. Le Goff, M. N. Rager, C. K.-M. Chan, V. W.-W. Yam and H. Amouri, *Organometallics*, **2013**, *32*, 4985–4992.
7. (a) T. K. Ronson, T. Lazarides, H. Adams, S. J. A. Pope, D. Sykes, S. Faulkner, S. J. Coles, M. B. Hursthouse, W. Clegg, R. W. Harrington and M. D. Ward, *Chem.-Eur. J.*, **2006**, *12*, 9299–9313; (b) V. Vajpayee, H. Kim, A. Mishra, P. S. Mukherjee, P. J. Stang, M. H. Lee, H. K. Kim and K.-W. Chi, *Dalton Trans.*, **2011**, *40*, 3112–3115; (c) X. Li, X. Zhao, J. Zhang and Y. Zhao, *Chem. Commun.*, **2013**, *49*, 10004–10006; (d) N. Zigon, N. Kyritsakas and M. W. Hosseini, *Dalton Trans.*, **2015**, *44*, 14204–14207; (e) Q.-Y. Zhu, L.-P. Zhou and Q.-F. Sun, *Dalton Trans.*, **2019**, *48*, 4479–4483; (f) Q.-Y. Zhu, L.-P. Zhou, L.-X. Cai, X.-Z. Li, J. Zhou and Q.-F. Sun, *Chem. Commun.*, **2020**, *56*, 2861–2864.
8. (a) K. Oisaki, Q. Li, H. Furukawa, A. U. Czaja and O. M. Yaghi, *J. Am. Chem. Soc.*, **2010**, *132*, 9262–9264; (b) C. I. Ezugwu, N. A. Kabir, M. Yusubov and F. Verpoort, *Coord. Chem. Rev.*, **2015**, *307*, 188–210; (c) Y. Dong, Y. Li, Y.-L. Wei, J.-C. Wang, J.-P. Ma, J. Ji, B.-J. Yao and Y.-B. Dong, *Chem. Commun.*, **2016**, *52*, 10505–10508.
9. T. Mocanu, C. I. Raț, C. Maxim, S. Shova, V. Tudor, C. Silvestru and M. Andruh, *CrystEngComm*, **2015**, *17*, 5474–5487.
10. T. Mocanu, L. Kiss, A. Sava, S. Shova, C. Silvestru and M. Andruh, *Polyhedron*, **2019**, *166*, 7–16.
11. I. Barbul, R. A. Varga, K. C. Molloy and C. Silvestru, *Dalton Trans.*, **2013**, *42*, 15427–15436.
12. A.-A. Someșan, I. Barbul, S. M. Vieriu, R. A. Varga and C. Silvestru, *Dalton Trans.*, **2019**, *48*, 6527–6538.
13. See, for example, selected references: (a) K. M. Fromm, J. L. Sagué Doimeadios and A. Y. Robin, *Chem. Commun.*, **2005**, 4548–4550; (b) A. Y. Robin, J. L. Sagué and K. M. Fromm, *CrystEngComm*, **2006**, *8*, 403–416; (c) T. Vig Slenters, I. Hauser-Gerspach, A. U. Daniels and K. M. Fromm, *J. Mater. Chem.*, **2008**, *18*, 5359–5362; (d) O. Gordon, T. Vig Slenters, P. S. Brunetto, A. E. Villaruz, D. E. Sturdevant, M. Otto, R. Landmann and K. M. Fromm, *Antimicrob. Agents and Chemother.*, **2010**, *54*, 4208–4218; (e) T. Vig Slenters, J. L. Sagué, P. S. Brunetto, S. Zuber, A. Fleury, L. Mirolo, A. Y. Robin, M. Meuwly, O. Gordon, R. Landmann, A. U. Daniels and K. M. Fromm, *Materials*, **2010**, *3*, 3407–3429, and references cited therein; (f) I. Chevrier, J. L. Sagué, P. S. Brunetto, N. Khanna, Z. Rajacic and K. M. Fromm, *Dalton Trans.*, **2013**, *42*, 217–231.
14. (a) J. Chen, A. Neels and K. M. Fromm, *Chem. Commun.*, **2010**, *46*, 8282–8284; (b) J. Chen, N. Voutier, J. Rajabi, A. Crochet, D. M. Bassani and K. M. Fromm, *CrystEng Comm*, **2017**, *19*, 5106–5113; (c) C. R. Kim, J. Ahn, T. H. Noh and O.-S. Jung, *Polyhedron*, **2010**, *29*, 823–826; (d) M. Tominaga, H. Ando, K. Ohara, T. Itoh and K. Yamaguchi, *Chem. Lett.*, **2018**, *47*, 315–31; (e) D. Kim, S. Park and O.-S. Jung, *Cryst. Growth Des.*, **2019**, *19*, 2019–2023.
15. (a) P. S. Brunetto, T. Vig Slenters and K. M. Fromm, *Materials*, **2011**, *4*, 355–367; (b) K. M. Fromm, *Appl. Organometal. Chem.*, **2013**, *27*, 683–687.
16. B. Cordero, V. Gomez, A. E. Platero-Prats, M. Reves, J. Echeverria, E. Cremades, F. Barragan and S. Alvarez, *Dalton Trans.*, **2008**, 2832–2838.
17. S. Alvarez, *Dalton Trans.*, **2013**, *42*, 8617–8636.
18. L. Yang, D. R. Powell and R. P. Houser, *Dalton Trans.*, **2007**, 955–964.
19. (a) J. Cirera, P. Alemany and S. Alvarez, *Chem.-Eur. J.*, **2004**, *10*, 190–207; (b) J. Cirera, E. Ruiz and S. Alvarez, *Chem.-Eur. J.*, **2006**, *12*, 3162–3167.
20. (a) E. Espinosa, I. Alkorta, J. Elguero and E. Molins, *J. Chem. Phys.*, **2002**, *117*, 5529–5542. (b) Á. Martín Pendás and J. Contreras-García, *Topological Approaches to the Chemical Bond*, Springer International Publishing, Cham, 2023, pp. 176–178.
21. P. Macchi, D. M. Proserpio and A. Sironi, *J. Am. Chem. Soc.*, **1998**, *120*, 13429–13435.
22. J. Klein, H. Khatabil, J.-C. Boisson, J. Contreras-García, J.-P. Piquemal and E. Hénon, *J. Phys. Chem. A*, **2020**, *124*, 1850–1860.
23. (a) E. R. Johnson, S. Keinan, P. Mori-Sánchez, J. Contreras-García, A. J. Cohen and W. Yang, *J. Am. Chem. Soc.*, **2010**, *132*, 6498–6506; (b) T. Lu and Q. Chen, *Chem.: Methods*, **2021**, *1*, 231–239.
24. C. R. Groom, I. J. Bruno, M. P. Lightfoot and S. C. Ward, *Acta Crystallogr. Sect. B Struct. Sci. Cryst. Eng. Mater.*, **2016**, *72*, 171–179.
25. Y. C. Ong, V. L. Blair, L. Kedzierski and P. C. Andrews, *Dalton Trans.*, **2014**, *43*, 12904–12916.
26. R. N. Duffin, V. L. Blair, L. Kedzierski and P. C. Andrews, *Dalton Trans.*, **2018**, *47*, 971–980.
27. S. Andleeb, Imtiaz-ud-Din, M. K. Rauf, S. S. Azam, I. Haq, M. N. Tahir and S. Ahmad, *Appl. Organomet. Chem.*, **2019**, *33*, e5061.
28. I. Kumar, P. Bhattacharya and K. H. Whitmire, *Organometallics*, **2014**, *33*, 2906–2909.
29. M. Qinghua, *CSD Commun.*, **2020**, refcode JUBQAB; CCDC 1975557.
30. (a) M. Pinsky and D. Avnir, *Inorg. Chem.*, **1998**, *37*, 5575–5582; (b) S. Alvarez and M. Llunell, *J. Chem. Soc. Dalton Trans.*, **2000**, 3288–3303; (c) D. Casanova, J. Cirera, M. Llunell, P. Alemany, D. Avnir and S. Alvarez, *J. Am. Chem. Soc.*, **2004**, *126*, 1755–1763.
31. A. A. Addison, T. N. Rao, J. Reedijk, J. van Rijn and G. C. Verschoor, *J. Chem. Soc. Dalton Trans.*, **1984**, 1349–1356.
32. V. V. Sharutin, I. V. Egorova, O. K. Sharutina, T. K. Ivanenko, Yu. V. Gatilov, N. A. Adonin and V. F. Starichenko, *Russ. J. Coord. Chem.*, **2003**, *29*, 462–467.
33. F. Cortés-Guzmán and R. F. W. Bader, *Coord. Chem. Rev.*, **2005**, *249*, 633–662.

34. V. V. Sharutin, V. S. Senchurin, O. K. Sharutina, Z. A. Starikova, S. A. Glazun and V. I. Bregadze, *Butlerov Commun.*, **2012**, 29(3), 51–56.
35. V. V. Sharutin, V. S. Senchurin and O. K. Sharutina, *Russ. J. Inorg. Chem.*, **2011**, 56, 1565–1567.
36. M. Nishio, *Phys. Chem. Chem. Phys.*, **2011**, 13, 13873–13900.
37. M. A. Spackman and D. Jayatilaka, *CrystEngComm*, **2009**, 11, 19–32.
38. Thermo Xcalibur Qual Browser, Thermo Fisher Scientific Inc., Waltham, MA, 02454, 2016.
39. G. M. Sheldrick, *Acta Crystallogr., Sect. A: Found. Adv.*, **2015**, 71, 3–8.
40. G. M. Sheldrick, *Acta Crystallogr., Sect. C: Struct. Chem.*, **2015**, 71, 3–8.
41. O. V. Dolomanov, L. J. Bourhis, R. J. Gildea, J. a. K. Howard and H. Puschmann, *J. Appl. Crystallogr.*, **2009**, 42, 339–341.
42. M. Llunell, D. Casanova, J. Cirera, P. Alemany and S. Alvarez, *SHAPE 2.1*, Universitat de Barcelona, Barcelona, Spain, 2013.
43. A. L. Spek, *Acta Crystallogr., Sect. D: Biol. Crystallogr.*, **2009**, 65, 148–155.
44. H. Putz, K. Brandenburg, DIAMOND – Crystal and Molecular Structure Visualization, Crystal Impact GbR, Kreuzherrenstr. 102, 53227 Bonn, Germany, 2022.
45. P. R. Spackman, M. J. Turner, J. J. McKinnon, S. K. Wolff, D. J. Grimwood, D. Jayatilaka and M. A. Spackman, *J. Appl. Crystallogr.*, **2021**, 54, 1006–1011.
46. (a) F. Neese, *WIREs Comput. Mol. Sci.*, **2012**, 2, 73–78; (b) F. Neese, *WIREs Comput. Mol. Sci.*, **2018**, 8, e1327; (c) F. Neese, F. Wennmohs, U. Becker and C. Riplinger, *J. Chem. Phys.*, **2020**, 152, 224108.
47. J. P. Perdew, K. Burke and M. Ernzerhof, *Phys. Rev. Lett.*, **1996**, 77, 3865–3868.
48. F. Weigend and R. Ahlrichs, *Phys. Chem. Chem. Phys.*, **2005**, 7, 3297–3305.
49. F. Weigend, *Phys. Chem. Chem. Phys.*, **2006**, 8, 1057–1065.
50. (a) S. Grimme, J. Antony, S. Ehrlich and H. Krieg, *J. Chem. Phys.*, **2010**, 132, 154104; (b) S. Grimme, S. Ehrlich and L. Goerigk, *J. Comput. Chem.*, **2011**, 32, 1456–1465.
51. D. Andrae, U. Häußermann, M. Dolg, H. Stoll and H. Preuß, *Theor. Chim. Acta*, **1990**, 77, 123–141.
52. B. Metz, H. Stoll and M. Dolg, *J. Chem. Phys.*, **2000**, 113, 2563–2569.
53. M. J. Frisch, G. W. Trucks, H. B. Schlegel, G. E. Scuseria, M. A. Robb, J. R. Cheeseman, G. Scalmani, V. Barone, G. A. Petersson, H. Nakatsuji, X. Li, M. Caricato, A. Marenich, J. Bloino, B. G. Janesko, R. Gomperts, B. Mennucci, H. P. Hratchian, J. V. Ortiz, A. F. Izmaylov, J. L. Sonnenberg, D. Williams-Young, F. Ding, F. Lipparini, F. Egidi, J. Goings, B. Peng, A. Petrone, T. Henderson, D. Ranasinghe, V. G. Zakrzewski, J. Gao, N. Rega, G. Zheng, W. Liang, M. Hada, M. Ehara, K. Toyota, R. Fukuda, J. Hasegawa, M. Ishida, T. Nakajima, Y. Honda, O. Kitao, H. Nakai, T. Vreven, K. Throssell, J. A. Montgomery, Jr., J. E. Peralta, F. Ogliaro, M. Bearpark, J. J. Heyd, E. Brothers, K. N. Kudin, V. N. Staroverov, T. Keith, R. Kobayashi, J. Normand, K. Ragahavachari, A. Rendell, J. C. Burant, S. S. Iyengar, J. Tomasi, M. Cossi, J. M. Millam, M. Klene, C. Adamo, R. Cammi, J. W. Ochterski, R. L. Martin, K. Morokuma, O. Farkas, J. B. Foresman and D. J. Fox, *Gaussian 09 Rev. E.01*, Gaussian Inc., Wallingford CT, USA, 2009.
54. (a) E. D. Glendening, C. R. Landis and F. Weinhold, *J. Comput. Chem.*, **2019**, 40, 2234–2241; (b) E. D. Glendening, J. K. Badenhoop, A. E. Reed, J. E. Carpenter, J. A. Bohmann, C. M. Morales, P. Karafiloglou, C. R. Landis and F. Weinhold, *NBO 7.0*, Theoretical Chemistry Institute, University of Wisconsin, Madison, WI, USA, 2018.
55. T. A. Keith, *AIMAll 19.10.12*, TK Gristmill Software, Overland Park, KS, USA, 2019.
56. T. Lu and F. Chen, *J. Comput. Chem.*, **2012**, 33, 580–592.

